

## Synthesis and Properties of Nd-substituted Bismuth Titanate Polycrystalline Thin Films with *a*-/*b*-axes Orientations

M. Kurachi<sup>1)</sup>, H. Matsuda<sup>2)</sup>, I. Honma<sup>2)</sup>, T. Iijima<sup>2)</sup>, H. Uchida<sup>1)</sup> and S. Koda<sup>1)</sup>

1) Faculty of Science and Engineering, Sophia University, 7-1, Kioi-cho, Tokyo 102-8554, Japan  
Fax: +81-3-3238-3361, e-mail: m-kurach@sophia.ac.jp

2) National Institute of Advanced Industrial Science and Technology, Tsukuba, 305 8568, Japan  
Fax: +81-29-861-5829, e-mail: hiro-matsuda@aist.go.jp

Polycrystalline  $\text{Bi}_{4-x}\text{Nd}_x\text{Ti}_3\text{O}_{12}$  (BNT,  $x=0.25, 0.50$  and  $0.75$ ) thin films with preferred *a*-/*b*-axes orientations were grown on  $\text{IrO}_2(101)/\text{SiO}_2/\text{Si}(100)$  substrates from chemical solution route. Insulating characters and ferroelectric properties in 250-nm-thick BNT ( $x=0.25$ ) thin films with *a*-/*b*-axes orientations were investigated at room temperature. Fair range in leakage current density of  $J=10^{-7}\sim 10^{-8}$  A/cm<sup>2</sup> at 100 kV/cm without the contribution from  $\text{Bi}_2\text{O}_3$  blocking layers and well-defined value of remnant polarization ( $2P_r=37$   $\mu\text{C}/\text{cm}^2$  at 400 kV/cm) were recorded. This range of  $J$  suggests the further possibility in reducing the film thickness suitable for low-voltage drive using *a*-/*b*-axes-oriented BLSF thin films.

Key words: BLSF, CSD, Orientation control, Polycrystalline film, Lanthanoids

### 1. INTRODUCTION

Bismuth layer structured ferroelectrics (BLSF) have been intensively investigated as the most competitive candidate materials for non-volatile ferroelectric random access memory (Nv-FeRAM) because of lead-free compositions and especially for high fatigue endurance [1]. Among wide structural and compositional range of BLSF, bismuth titanate  $\text{Bi}_4\text{Ti}_3\text{O}_{12}$  (BIT) crystal has attracted particular interest due to that large value of spontaneous polarization  $P_s$  was reported [2]. In the pseudo-orthorhombic BIT unit with the lattice parameters *a*, *b* and *c* of 0.5448, 0.5410 and 3.284 nm, respectively [3], the ferroelectric activity appears with spontaneous polarization  $P_s$  of 50 and 4  $\mu\text{C}/\text{cm}^2$  along *a*- and *c*-axis, respectively [4]. Recently, in addition, modifications into BIT lattice by lanthanoids such as La, Nd and Sm have been conducted along the site engineering concept and remarkable improvement of ferroelectric polarization properties were reported [5-7]. Among them,  $\text{Bi}_{4-x}\text{Nd}_x\text{Ti}_3\text{O}_{12}$  (BNT) has been receiving great attention because of its superior value of remnant polarization in epitaxial and polycrystalline films [8-9]. Furthermore, the possibility of the enhancement in  $P_s$  by Nd substitution was suggested [10].

The *a*-/*b*-axes-oriented BIT-type epitaxial thick films have been achieved by utilizing bottom electrode layers of simple perovskite [11] and rutile-type structure [12], in order to align the polar-*a*-axis along the film normal. In addition, polycrystalline  $\text{Bi}_{4-x}\text{Pr}_x\text{Ti}_3\text{O}_{12}$  (BPT) thick films with polar-*a*-axis orientation grown on the oxidized  $\text{IrO}_2$  layers exhibited almost complete value of spontaneous polarization measured in single crystalline BIT [13].

However, the BLSF films of *a*-/*b*-axes orientations with the film-thickness below 400 nm have never been reported so far [10-14], because  $\text{Bi}_2\text{O}_3$  blocking layers align parallel to the applied electric field [15], and the electric conductivity parallel to  $\text{Bi}_2\text{O}_3$  layers is higher

than that of perpendicular direction [16]. And also larger film thickness causes too high drive voltage. Therefore, it is significant to evaluate insulating character of BNT thin films with the electrical field parallel to the  $\text{Bi}_2\text{O}_3$  layers using *a*-/*b*-axes orientations for practical applications.

In present work, we report the electrical properties in BNT polycrystalline thin films with *a*-/*b*-axes orientations and the film thickness of 250 nm.

### 2. EXPERIMENTAL PROCEDURE

(101)-oriented  $\text{IrO}_2$  conducting oxide layers were deposited on  $\text{SiO}_2/\text{Si}(100)$  wafers by reactive RF sputtering as bottom electrodes with the thickness of 100 nm. Coating solutions with nominal compositions  $\text{Bi}_{4-x}\text{Nd}_x\text{Ti}_3\text{O}_{12}$  (BNT,  $x=0.25, 0.50$  and  $0.75$ ) were prepared by dissolving hygroscopic starting materials of Bi-acetate, Nd-acetate-hydrate and Ti-iso-propoxide (Aldrich, 99.99+, 99.9 and 99.999 % in purity, respectively) in anhydrous 2-methoxyethanol (99.8 %, Aldrich). The thermal decomposition behavior of the coating solution was examined in air with the rate of  $10$   $^\circ\text{C}\cdot\text{min}^{-1}$  by thermo-gravimetry and differential thermal analysis [(TG-DTA), Thermoplus TG8120, Rigaku]. The coating solutions were spin-coated on the substrates, followed by a calcination process for direct crystallization of BNT on a hot-plate at  $530\sim 570$   $^\circ\text{C}$  repeatedly. Subsequent annealing by rapid thermal annealing was performed at  $720$   $^\circ\text{C}$  for grain growth. The crystal structure and orientation behavior of deposited films were investigated by x-ray diffraction [(XRD), X'pert Pro, PANalytical] of  $\text{CuK}\alpha$  radiation. Film thickness and surface morphology were observed by field-emission scanning electron microscope [(FE-SEM), S-5000, Hitachi]. Electrical property measurements were conducted at room temperature with ferroelectric testing system [RT-66A, Radiant] and leakage current density measurement [4140B, Agilent

Technology], after depositing Pt top electrode layers with the diameter of 200  $\mu\text{m}$  through metal mask.

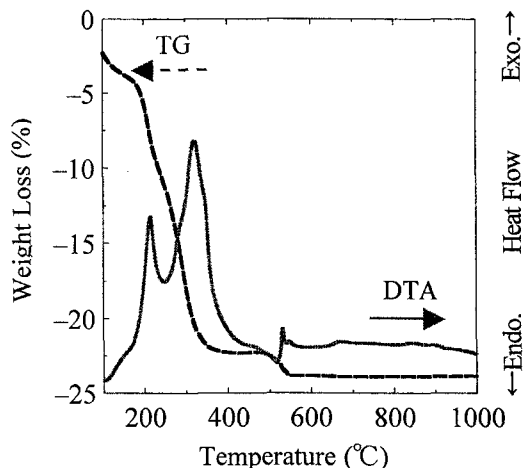


**Fig.1:** TG-DTA curves of BNT( $x=0.25$ ) powder.

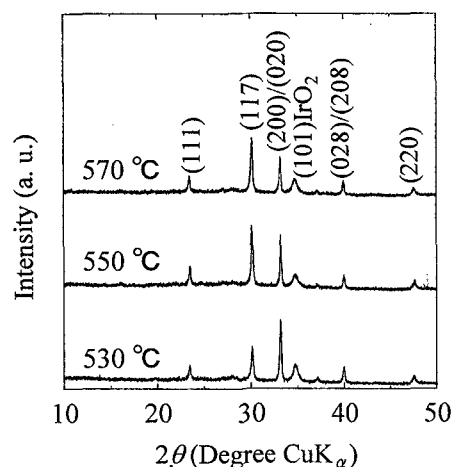
### 3. RESULTS AND DISCUSSION

Figure 1 shows the TG-DTA curves of BNT( $x=0.25$ ) powders derived from chemical solution by drying at 150  $^{\circ}\text{C}$  in air. The TG-DTA curves revealed complete thermal decomposition of the solution was fulfilled at about 530  $^{\circ}\text{C}$ . Therefore, the crystallization temperature ( $T_{\text{cr}}$ ) was decided over 530  $^{\circ}\text{C}$  for inheriting the atomic arrangement of  $\text{IrO}_2$  layer during crystallization in BNT films.

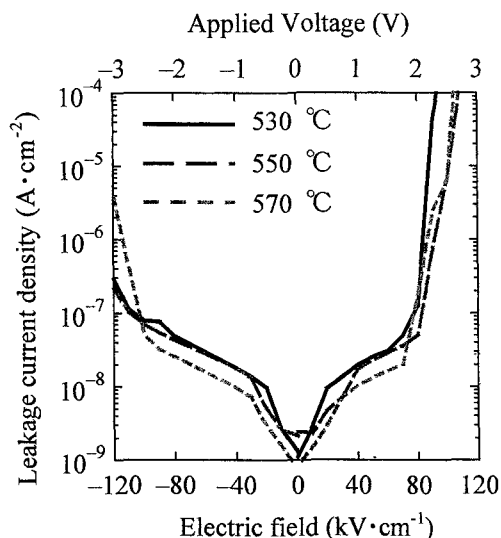
Figure 2 shows the XRD profiles of BNT ( $x = 0.25$ ) films with varying  $T_{\text{cr}}$ . The BNT film of  $T_{\text{cr}} = 530$   $^{\circ}\text{C}$  exhibited dominant (200)/(020) orientations surpassing (117) orientation, while the films of higher  $T_{\text{cr}} = 550$  and 570  $^{\circ}\text{C}$  exhibited higher intensity of (117) than those of (200)/(020). In addition, not shown here, but films of  $T_{\text{cr}}$  under 500  $^{\circ}\text{C}$  exhibited dominant (117) orientation with some *c*-axis orientation components. These different orientation behaviors upon  $T_{\text{cr}}$  might derive from the rates of grain growth among (200)/(020) and (117) planes. At this range of  $T_{\text{cr}}$ , these rates of grain growth might be the most competitive, and which required very narrow process window within  $\Delta T_{\text{cr}} = 20$   $^{\circ}\text{C}$  for growing the preferred *a*/*b*-axes-oriented BNT films.

Figure 3 shows the room temperature characteristics of leakage current density ( $J$ ) as function of electric field ( $E$ ) in BNT ( $x=0.25$ ) thin films with the film thickness of 250 nm (solid, dashed and dotted lines respectively indicate  $T_{\text{cr}} = 530, 550$  and 570  $^{\circ}\text{C}$ ). All of 250-nm-thick BNT films with different orientations exhibited similarly fair values of  $J=10^{-7}$ – $10^{-8}$   $\text{A}/\text{cm}^2$ , although relatively higher  $J$  was observed in the film with *a*/*b*-axes orientations. This range of  $J$  suggests the further possibility in reducing the film thickness suitable for low-voltage drive without the contribution on insulating property from  $\text{Bi}_2\text{O}_2$  blocking units along the DC electrical field. Relatively poor values of DC breakdown field ( $\sim 100$   $\text{kV}/\text{cm}$ ), on the other hand, were observed. These values should be improved for practical applications.

Figure 4(a) shows the room temperature polarization



**Fig.2:** XRD profiles of  $\text{Bi}_{3.75}\text{Nd}_{0.25}\text{Ti}_3\text{O}_{12}$  ( $T_{\text{cr}} = 530$ – $570$   $^{\circ}\text{C}$ ) polycrystalline thin films deposited on  $(101)\text{IrO}_2/\text{SiO}_2/\text{Si}$ .



**Fig.3:** The room temperature leakage current density and electric field ( $J$ - $E$ ) characteristics in  $\text{Bi}_{3.75}\text{Nd}_{0.25}\text{Ti}_3\text{O}_{12}$  ( $T_{\text{cr}} = 530$ – $570$   $^{\circ}\text{C}$ ) polycrystalline thin films with the thickness of 250 nm.

electric field ( $P$ - $E$ ) hysteresis loops at a maximum  $E=640$   $\text{kV}/\text{cm}$  at 50 Hz and Fig. 4(b) shows saturation curves of remnant polarization ( $P_r$ ) and coercive electric field ( $E_c$ ) in BNT ( $x=0.25$ ) thin film of  $T_{\text{cr}}=530$   $^{\circ}\text{C}$ . Good saturation behaviors of  $P_r$  and  $E_c$  were achieved below 10 V. Since the thermal expansion coefficient of Si is much smaller than that of oxide ionic crystals, in-plane tensile strain is introduced during cooling and leads to *a*/*b*-axes mixed orientations [17]. Considering the continuous saturation curves, the rotation of *a*/*b*-domains was unlikely even at  $E>700$   $\text{kV}/\text{cm}$ . The somewhat poor value of observed  $P_r$ , compared with that of BIT single crystals may be derived from *a*/*b*-axes mixed orientations.

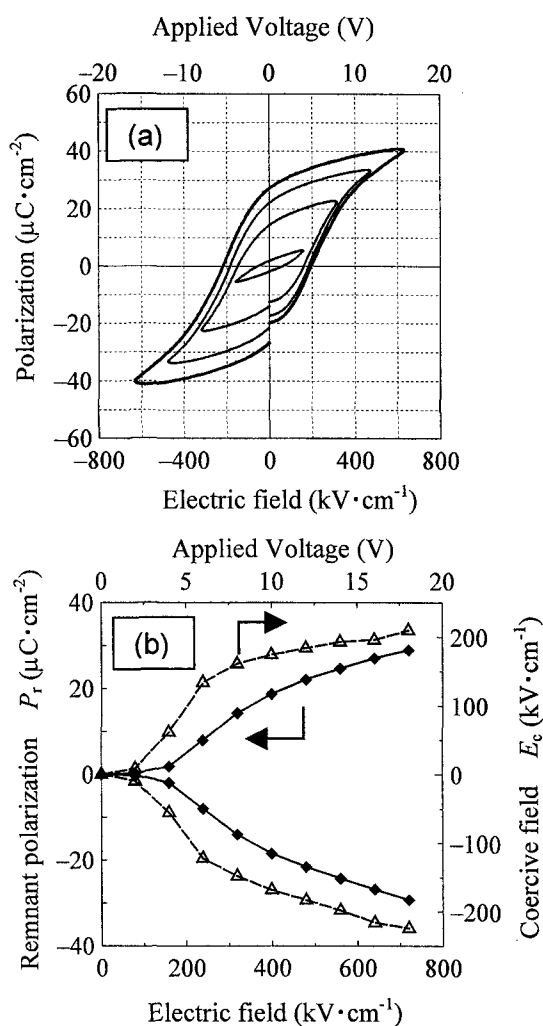


**Fig.4:** Room temperature ferroelectric properties in 250 nm-thick BNT thin film of  $x=0.25$  and  $T_{cr}=530$  °C. (a)  $P$ - $E$  hysteresis loops and (b) Saturated curves of  $P_r$  and  $E_c$ .

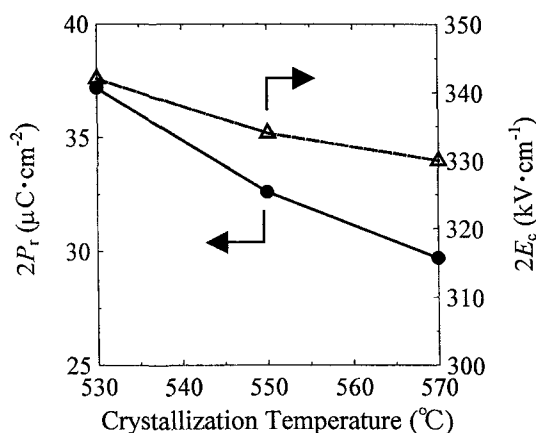


**Fig.5:** The  $T_{cr}$  dependence of measured  $2P_r$  and  $2E_c$  under the electric field of 400 kV/cm (10 V) at 50 Hz in 250 nm-thick BNT( $x=0.25$ ) films.

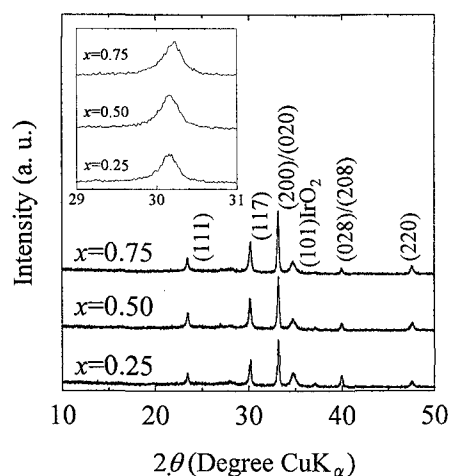


**Fig.6:** XRD profiles of 250 nm-thick BNT ( $x=0.25$ -0.75) polycrystalline thin films deposited on  $(101)\text{IrO}_2/\text{SiO}_2/\text{Si}$ .

**Table.1:** Ferroelectric polarization properties of 250 nm-thick BNT films.

$x$	$2P_r$ ( $\mu\text{C}\cdot\text{cm}^{-2}$ )	$2E_c$ ( $\text{kV}\cdot\text{cm}^{-1}$ )
0.25	37	337
0.50	31	320
0.75	25	296

Figure 5 shows  $T_{cr}$  dependence of  $2P_r$  and  $2E_c$  under  $E=400$  kV/cm (10 V) at 50 Hz in 250 nm-thick BNT ( $x=0.25$ ) thin films. The maximum values were  $2P_r=37$   $\mu\text{C}/\text{cm}^2$  and  $2E_c=342$  kV/cm for  $T_{cr}=530$  °C, respectively. The values of  $2P_r$  continuously decreased with increasing  $T_{cr}$ . This trend may reflect the orientation behavior upon  $T_{cr}$ .

Since most of reported works on BNT thin films have been concentrated in Nd-substitution content  $x$  in the range of  $0.50 < x < 0.85$ , [8-10,18,19] we also investigated ferroelectric properties in BNT thin films of  $x=0.50$  and 0.75 with preferred  $a$ - $b$ -axes orientations

Figure 6 shows XRD profiles of BNT films with Nd-substitution content  $x$ . The inset shows the monotonous shift of (117) peak position toward higher  $2\theta$  with increasing  $x$ , indicating that Nd ion was incorporated into BIT lattice. Similar orientation behaviors of BNT thin films were achieved for all of  $x$ . This result suggests that the concept of long-range lattice matching between oblong (101) plane in rutile-type structure and  $a$ - $c$ / $b$ - $c$  planes in BIT is valid for the present wide range of  $x=0.25$ -0.75. We found that, furthermore, the process window of crystallization for preferred  $a$ - $b$ -axes orientations expanded to  $\Delta T_{cr}=50$

and 60 °C for  $x=0.50$  and  $0.75$ .

Table I shows a list of  $2P_r$  and  $2E_c$  in 250 nm-thick BNT thin films of  $x=0.25$ ,  $0.50$  and  $0.75$  under  $E=400$  kV/cm (10 V). Similarly good saturation behaviors of  $P_r$  and  $E_c$  were achieved below 10 V for all  $x$ . The  $2P_r$  and  $2E_c$  values decreased continuously with increasing  $x$ . Based on thermal and structural analyses for BNT crystalline powders, we have observed monotonous decreases both in Curie temperature  $T_c$  and orthorhombic anisotropy  $a/b$  with increasing  $x$ . [20]. The observed monotonous decrease in  $2P_r$  of BNT thin films with the increase of  $x$  may be related to the bulk properties of  $T_c$  and  $a/b$  in BNT crystal.

#### 4. CONCLUSION

We synthesized polycrystalline BNT ( $x=0.25$ ,  $0.50$  and  $0.75$ ) thin films with *a*-*b*-axes orientations and the thickness of 250 nm on IrO<sub>2</sub>(101)/SiO<sub>2</sub>/Si(100) substrates by chemical solution deposition method. By optimizing the heat treatment conditions, low leakage current density of  $J=10^7\sim 10^8$  A/cm<sup>2</sup> at 100 kV/cm was achieved in BNT ( $x=0.25$ ) thin films without the Bi<sub>2</sub>O<sub>2</sub> blocking units along the DC electrical field due to the *a*-*b*-axes orientations. From the measurement of ferroelectric properties at room temperature, well-saturated *P*-*E* hysteresis loops and fair value of remnant polarization ( $2P_r=37$  μC/cm<sup>2</sup> at 400 kV/cm) were measured in BNT thin films of  $x = 0.25$ . These results could promote the application of lead-free BLSF thin films with *a*-*b*-axes orientations for Nv-FeRAM devices.

#### ACKNOWLEDGMENTS

One of the authors (H. M.) wishes to acknowledge for financial support of Grant-in-Aid for Young Scientist (B) from The Ministry of Education, Culture, Sports, Science and Technology of Japan (Grant No.14750563).

#### REFERENCES

- [1] J. F. Scott and C. A. Paz. de Araujo, *Science*, **246**, 1400 (1989).
- [2] H. Irie, M. Miyayama and T. Kudo, *J. Appl. Phys.*, **90**, 4089 (2001).
- [3] A. D. Rac, J. G. Thompson, R. L. Withers and A. C. Willis, *Acta. Crystallogr.*, **B46**, 4089 (1990).
- [4] S.E. Cummins and L. E. Cross, *J. Appl. Phys.*, **39**, 2268 (1968).
- [5] B. H. Park, B. S. Kang, S. D. Bu, T. W. Noh, J. Lee and W. Jo, *Nature*, **401**, 682 (1999).
- [6] H. Uchida, H. Yoshikawa, I. Okada, H. Matsuda, T. Iijima, T. Watanabe and H. Funakubo, *Jpn. J. Appl. Phys.*, **41**, 6820 (2002).
- [7] U. Chon, K. B. Kim, H. M. Jang and G. C. Yi, *Appl. Phys. Lett.*, **79**, 3137 (2001).
- [8] T. Kojima, T. Sakaki, T. Watanabe, H. Funakubo, K. Saito and M. Osada, *Appl. Phys. Lett.*, **80**, 2746 (2002).
- [9] H. Uchida, H. Yoshikawa, I. Okada, H. Matsuda, T. Iijima, T. Kojima, T. Watanabe and H. Funakubo, *Appl. Phys. Lett.*, **81**, 2229 (2002).
- [10] T. Watanabe, T. Kojima, H. Uchida, I. Okada and H. Funakubo, *Jpn. J. Appl. Phys.* **43**, L309 (2004).
- [11] H. N. Lee, D. Hesse, N. Zakharov and U. Goesele, *Science* **296**, 2006 (2002).
- [12] T. Watanabe, H. Funakubo, K. Saito, T. Suzuki, M. Fujimoto, M. Osada, Y. Noguchi and M. Miyayama, *Appl. Phys. Lett.*, **81**, 1660 (2002).
- [13] H. Matsuda, S. Ito and T. Iijima, *Appl. Phys. Lett.*, **83**, 5023, (2003).
- [14] K. Kato, D. Fu, K. Suzuki, K. Tanaka, K. Nisizawa and T. Miki, *Appl. Phys. Lett.*, **84**, 3771 (2004).
- [15] H. S. Shulman, M. Tstrof, D. Damjanovic and N. Setter, *J. Am. Ceram. Soc.*, **79**, 3124 (1996).
- [16] M. Takahashi, Y. Noguchi and M. Miyayama, *Jpn. J. Appl. Phys.*, **11B**, 7053 (2002).
- [17] K. Lee, K. S. Lee and S. Baik, *J. Appl. Phys.*, **90**, 6327 (2001).
- [18] M. Yamada, N. Iizawa, T. Yamaguchi, W. Sakamoto, K. Kikuta, T. Yogo, T. Hayashi and S. Hirano, *Jpn. J. Appl. Phys.*, **42**, 5222 (2003).
- [19] A. Garg, and Z. H. Barber, M. Dawber, J. F. Scott, A. Snedden and P. Lightfoot; *Appl. Phys. Lett.*, **83**, 2414 (2003).
- [20] H. Matsuda, M. Kurachi, H. Uchida, T. Watanabe, T. Iijima, S. Koda, and H. Funakubo, submitted to *Jpn. J. Appl. Phys.*

(Received December 23, 2004; Accepted January 31, 2005)